World Journal of Otorhinolaryngology-Head and Neck Surgery (2018) 4, 50–56

Available online at www.sciencedirect.com

ScienceDirect

journal homepage: www.keaipublishing.com/WJOHNS; www.wjent.org

Research Paper

Morphological evaluation using MRI of the olfactory filaments (fila) in a post-traumatic olfactory rat model

Zhi-Fu Sun [a], Xing Gao [a], Jayant M. Pinto [b], Yin He [c], QingXian Yang [d], Jun Tian [e], Qian-Wen Lv [a], Yong-Xiang Wei [a,*]

[a] *Department of Otorhinolaryngology Head and Neck Surgery, Beijing Anzhen Hospital, Capital Medical University, Beijing 100029, China*
[b] *Section of Otolaryngology Head and Neck Surgery, Department of Surgery, The University of Chicago, Chicago, IL 60647, USA*
[c] *Department of Emergency, Beijing Anzhen Hospital, Capital Medical University, Beijing 100029, China*
[d] *Department of Radiology, Penn State College of Medicine, PA 17033, USA*
[e] *Department of Otorhinolaryngology Head and Neck Surgery, The First Hospital of Shanxi Medical University, Taiyuan 030001, China*

Received 6 February 2018; accepted 2 March 2018
Available online 11 May 2018

KEYWORDS
MicroMRI;
Olfactory fila;
Olfactory bulb;
Post-traumatic olfactory dysfunction model;
Rat

Abstract *Objective:* To investigate whether magnetic resonance imaging (MRI) can be used to directly assess olfactory bulb (OB) lesions and quantify the associated morphological changes of olfactory filaments (OF), also known as fila, in an *in vivo* OB-lesion rat model of the brain.
Methods: A surgical group ($n = 5$) of male Sprague–Dawley rats was subjected to the unilateral damage of the OB by a steel needle. The control group ($n = 5$) did not receive surgery. To assess olfactory system injury *in vivo*, T2-weighted MRI images were acquired in an oblique plane at a 30° angle from transverse plane one day after surgery. These brain regions were also assessed in the controls. The olfactory function was evaluated using the buried food pellet test (BFPT) 5 days before and after surgery.
Results: The OF could be clearly observed on the MRI images from all animals. The left and right OF mean lengths (mm) were similar in the control group (0.81 ± 0.18 *vs* 0.89 ± 0.17, $P > 0.05$). In the surgical group, the OB was partially injured in all rats. These rats did not show

* Corresponding author.
E-mail address: weiyongxiang@vip.sina.com (Y.-X. Wei).
Peer review under responsibility of Chinese Medical Association.

Production and Hosting by Elsevier on behalf of KeAi

https://doi.org/10.1016/j.wjorl.2018.03.004

differences in OF length between left- and right-side (0.83 ± 0.18 *vs* 0.93 ± 0.24, $P > 0.05$) at the time of measurement. The time (sec) required to find the food pellets in the BFPT was longer after than before the surgery (83.80 ± 34.37 *vs* 231.44 ± 53.23, $P < 0.05$).
Conclusions: MicroMRI may be a feasible tool to evaluate the OF and OBs in rat models. The unilateral partial OB lesion model appears to be an effective post-traumatic olfactory dysfunction model.

Introduction

The olfactory filaments (OFs), also known as olfactory fila, are among the most important structures in the olfactory system and play a key role in connecting peripheral olfactory neurons to the central nervous system. The OFs are formed by a cluster of hundreds to many thousands of olfactory receptor axons bundled together within olfactory ensheathing cells. The collection of such receptor cells makes up the olfactory nerve (cranial nerve I). The axons of these receptor cells form the outermost layer of the olfactory bulb (OB) and enter into the next layer of the bulb, where they synapse within spherical structures, termed glomeruli, with the dendrites of the bulb's major projection neurons, the mitral and tufted cells.[1] These cells in turn project to a number of higher brain regions.

In addition to conveying the axons that transmit olfactory receptor signals, the OFs also regulate the function and growth of various kinds of cells of the olfactory epithelium. For example, after the OFs are severed, the olfactory epithelium thins and the number of its cells decreases; as recovery from damage occurs, the epithelium thickens and the cells multiply.[2] The OFs, under some circumstances, allow for the transport of xenobiotics (including viruses, drugs, and nanoparticles) directly from nose into the brain.[3–7] These phenomena, as well as the unique capacity of the olfactory nerve and other elements of the olfactory epithelium to regenerate, have led to a plethora of research studies of the OFs in recent years.[8,9] For example, the OFs are now widely used as a model in animal experiments to explore neuronal regeneration.[10]

The classic animal model of post-traumatic olfactory dysfunction involves transection of the OFs.[11–17] A number of animal models of olfactory disorders have focused on the OF, including those related to factors that damage the olfactory pathways, including inflammatory processes, viruses, and toxins.[18–22] In human studies, researchers have found that the status of the axons of the olfactory neurons provides useful information about the overall condition of the peripheral olfactory system and may improve the interpretation of the diagnostic implications of mucosal biopsies.[23] Thus, the OFs play a vital role in the study of smell disorders. However, OFs are vulnerable and difficult to directly research. To date, horseradish peroxidase (HRP) staining and manganese (Mn^{2+}) imaging represent two of the most frequently used methods to evaluate the OFs,[24,25] with HRP staining acting as an indirect indicator of lesions in the olfactory neuron axon and Mn^{2+} acting as a direct indicator for magnetic resonance imaging (MRI) assessment. However, these methods have limitations. For example, the use of HRP precludes evaluations of the function of the OFs because this procedure requires animal sacrifice, and Mn^{2+} is associated with biological toxicity. Although many animals can tolerate this ion, it may influence the recovery process and produce confounding results.[26,27] Despite the fact that researchers have achieved limited success with the use of Thallium^{201} (^{201}TI) imaging or transgenic animals in evaluating the function or morphology of the OFs,[28,29] these methods also have drawbacks. Transgenic mice also have to be sacrificed to examine the olfactory system.[15,17,30,31] And ^{201}TI, which has been successfully used in the clinic as an effective method of evaluating the function of the olfactory system in Japan,[32] is expensive. Moreover, the OFs are so small that it is difficult to successfully image them.

To overcome these obstacles, an economical and effective method is needed that can repeatedly and directly record the OFs without affecting its natural recovery process. Such a method would be very helpful in a variety of olfactory studies. One method, which is explored in this study, is MRI. MRI is a highly versatile imaging technique that has been widely used in clinics and research since its early development in the 1970s.[33] Chang and Jang[34] attempted to use MRI to distinguish the five distinct layers of the hamster OB more than twenty years ago. However, this study was limited to hamster models and did not adequately display the OF. With the rapid development of animal imaging technology in recent years, MRI can easily resolve volumes less than 1 μm, which indicates that the OFs can be directly imaged in rats. To date, olfactory-related research has not performed MRI experiments to directly image the OF. Thus, whether microMRI can be applied to directly display the OFs *in vivo* in rats requires investigation. This study explored this concept and aimed to utilize MRI as a new *in vivo* method for evaluating the OFs in a transectional OF model.

Materials and methods

Animals

Male Sprague–Dawley rats (body weight of ~300 g) were obtained from Vital River (Vital River SLC, Beijing, China) and housed in a 22 °C air-conditioned room with a 12/12 h light/dark cycle. They were provided adlibitum with a

standard pellet diet and water. The Capital Medical University Animal Experiment Committee approved all animal procedures in advance (No. AEEI-2016-059).

Surgical procedures

Five rats were anesthetized with sodium pentobarbital (60 mg/kg) through intraperitoneal injection and then placed under a stereomicroscope. A midline incision was performed to expose the anterior aspect of the skull. Then, the underlying OB was exposed using a dental drill and microforceps. With the aid of a dissecting microscope, a curved and partially blunted 23-gauge hypodermic needle was used to damage the OB on the left side. A sham operation with no damage was performed on the right side. Perfusion of cold sterile saline into the exposed area served to minimize bleeding throughout the surgery. After surgery, the skin over the exposed region was closed using stainless steel wound clips. One day after surgery, the rats were scanned by microMRI.

Olfactory function test

A buried food pellet test (BFPT) was used to evaluate the olfactory function of rats 5 days before and after the surgery. This behavioral test has been used numerous times to assess olfactory function.[35–39] On test days, the rats were restricted to 0.5 g of food per day. Water was available adlibitum. BFPT training and testing were performed in a 55 cm × 30 cm × 35 cm closed non-transparent container whose flooring was covered with 5 cm thick rat bedding material. A food pellet was buried approximately 1 cm below the surface at random sites during each trial. The latency to find the food (forelimbs clinging to the food pellet or gripping it with teeth) after introduction into the test situation was recorded.[40] If the rat did not find the food pellet within 5 min, the latency was recorded as 300 s. The average latencies for each of 5 days of testing was used for analysis.

MRI

All of the OF images of this study were obtained at the position of oblique coronal after the median sagittal orientation (Fig. 1). The red oblique bars show oblique coronal direction of scanning.

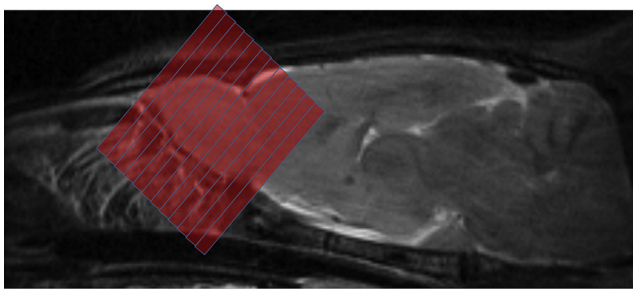

Fig. 1 OB and cribriform plate observed *in vivo* via MRI on the orientation of median sagittal. The red oblique bars is the oblique coronal direction of scanning method applied in this study to observe OFs.

The details of the scanning are as follows: each animal was anesthetized in the induction chamber using isoflurane, and then fixed in a prone position. High-resolution MRI was performed (1 day after the surgery in surgery group). Images were acquired on a PharmaScan® 7T/16 horizontal magnet (Bruker Co., Germany). The rat was placed in a custom-designed plastic stereotaxic holder with a tooth bar to immobilize the head. The anesthesia (1.5%—2.0% isoflurane mixed with air) was delivered through a nose-cone. The animal's heart rate and respiration were monitored during the entire experiment. Time series, T1-weighted and T2-weighted MRI images, were acquired by a rapid acquisition relaxation enhancement (RARE) sequence. The coronal T1-weighted images were obtained in the horizontal direction at a counter-clockwise 30° angle (Fig. 1) with the repetition time/echo time = 1300/39 ms. The T2-weighted images were obtained using the following parameters: repetition time/echo time = 3000/45 ms; flip angle 180; internumber of signals acquired, 10; matrix size = 384 × 384, pixel resolution 91 × 91 mm/pixel; FOV 3.5 cm × 3.5 cm; number of slices = 15 and slice thickness, 0.5 mm (no gaps); RARE factor of 8, 2D volumes of 91-μm isotropic spatial resolution were obtained every 20 min.

MRI data analysis

Image J software (Wayne Rasband, National Institutes of Health, USA) was used to analyze the OF length of the rats. Images that accurately displayed the OFs were selected, and the length of the OFs from the nasal cavity to the OB were measured.

Statistical analysis

SPSS (version 22 for Windows) was used for the statistical analysis. Means and standard deviations were used to describe continuous variables. The mean value of each group was compared within the group using analysis of variance after normality and homogeneity of variance was verified. A P value of 0.05 or less was considered statistically significant.

Results

OFs could be clearly seen on all of the MRI images. Three pairs of OFs were observed in three of the rats, and four pairs of OFs were observed in two of the rats in control group. Significant differences were not observed between the mean lengths (mm) of the left and right OFs in the five rats of the control group (0.81 ± 0.18 *vs* 0.89 ± 0.17, $P > 0.05$). Although observing the entire OF on a single plane is difficult because of its irregularity, OFs that pass through the ethmoid foramen can be easily observed in oblique coronal images. In the surgical group, three pairs of OFs in three rats and four pairs of OFs in two rats were observed under MRI. Similar to the controls, the mean left- and right-side lengths (mm) of the OFs did not differ in the operated animals (0.83 ± 0.18 *vs* 0.93 ± 0.24, respectively, $P > 0.05$). In rats that underwent surgery, the OB was damaged in all cases ($n = 5$). The pre- and post-operative BRPT (sec) latencies differed significantly in the surgical

group (83.80 ± 34.37 *vs* 231.44 ± 53.23, respectively, $P < 0.05$).

OFs in control group *in vivo* by MRI

The images show pairs of OFs originating from the olfactory epithelium and traveling through the foramina in the cribriform plate to connect with the OB (Fig. 2).

OFs in the surgical group imaged with MRI *in vivo*

All of the OFs were intact well after the surgery process. We did note partial injury of the OB; only rarely was OF damage observed after surgery ($n = 5$, Fig. 3).

BFPM latencies before and after surgery

The mean (SEM) latencies to find the buried food pellets before and after surgery are shown in Fig. 4. It is apparent that the rats who had undergone the surgery had difficulty finding of the food pellets.

The mean length of the OFs in the control and surgical groups

The mean length (mm) of the left and right OFs in control rats were 0.81 ± 0.18 and 0.89 ±0.17, respectively ($P > 0.05$). The mean length (mm) of the damaged side (left) and normal side (right) in the surgical group were 0.83 ± 0.18 and 0.93 ± 0.24, respectively ($P > 0.05$). Thus, no significant difference was apparent in the OF lengths between the left side and right sides of either group (Fig. 5, $P > 0.05$).

Discussion

This pilot experiment shows, for the first time, that the OFs of rats can be visualized using *in vivo* microMRI. Further development of this technology may allow for the evaluation of the morphology of the OFs in rats, thereby increasing the range of potential questions that can be addressed. As an example, we applied this method to verify the OB-lesion model. Our data suggest that damage to one OB has no impact on the length of the OFs on either side of nose, even though it produced a significant increase in BFPT latencies.

The morphological integrity of the OFs is critical for normal olfactory function. Researchers have noticed that OFs are an important route, in both humans and animals, for the unintended entrance of xenobiotics into the brain.[3,4,41–43] Injury to the olfactory nerve fibers at the site where the nerve filaments traverse the cribriform plate and project to the OB is one of the most common causes of olfactory loss related to trauma.[44–46] The status of OFs reflects, in large part, the overall condition of the olfactory system and is known to correlate with olfactory function.[23] Animal experiments are essential for studying the mechanisms of olfactory disorders and the development of therapeutic methods, given the impossibility of performing invasive studies in humans. Nonetheless, research in rodents has been challenging because of the small size and location of the filaments. Previous researchers have tried to use HRP,[24] Mn^{2+},[25] and ^{201}Tl,[28] to visualize and study the

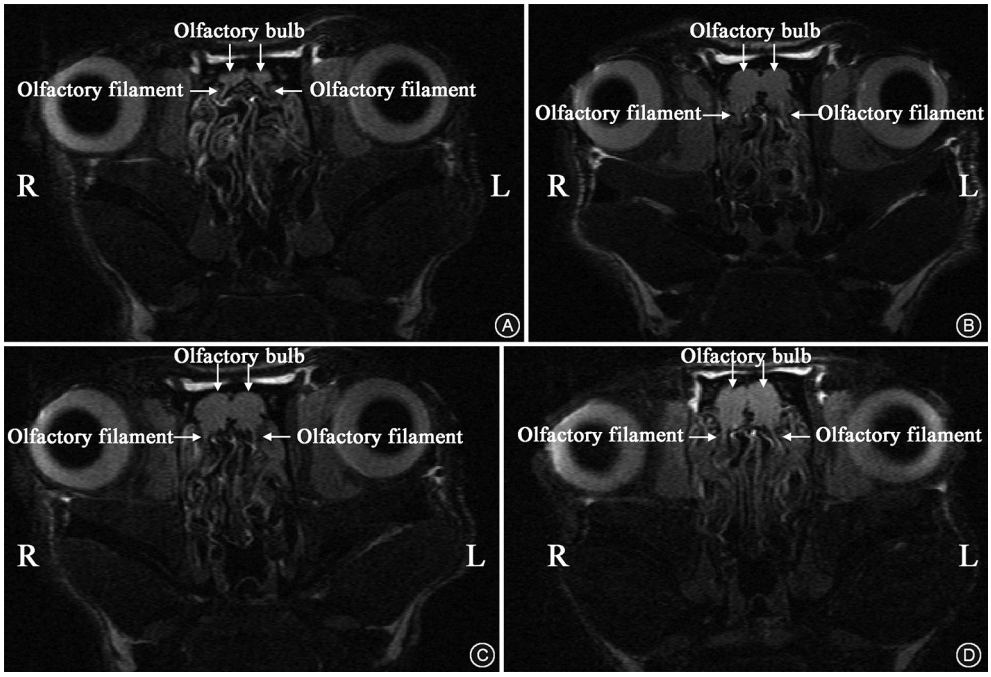

Fig. 2 Morphology of the olfactory system obtained with T2-weighted images in the oblique coronal direction on different scanning planes in the control group. The OB is indicated by the vertical arrow, and OF is indicated by the horizontal arrow. The images clearly show pairs of OFs originating from the olfactory epithelium and then synapsing with the OB. A, B, C, and D in Fig. 2 are different planes from the anterior to the posterior OB.

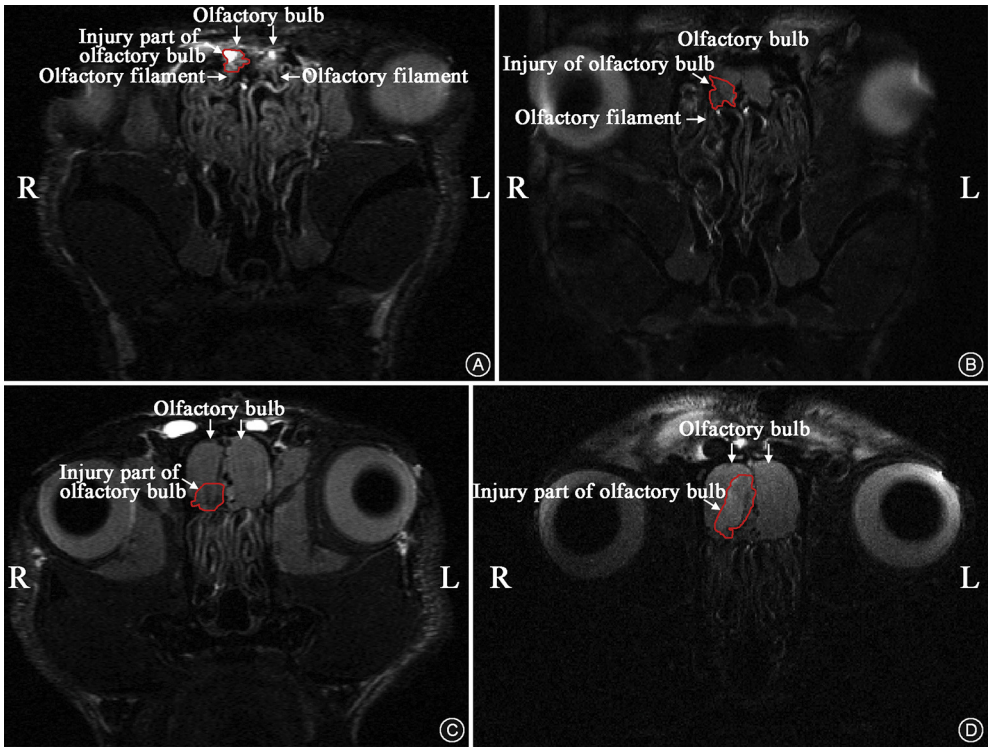

Fig. 3 Morphology of the OBs and OFs in the oblique coronal direction on different scanning planes in the surgical group: OBs are indicated by the vertical arrow and OFs are indicated by the horizontal arrow. A, B, C, and D in Fig. 3 are different scanning planes from the anterior to the posterior OBs. In the surgical group, the damaged side is on the left and the normal side is on the right. The injured area of the OB is circled in line. The OFs shown in the image were well connected with the OBs. The injured area of the OB is visible, and normal OF length and structure of both sides are observed.

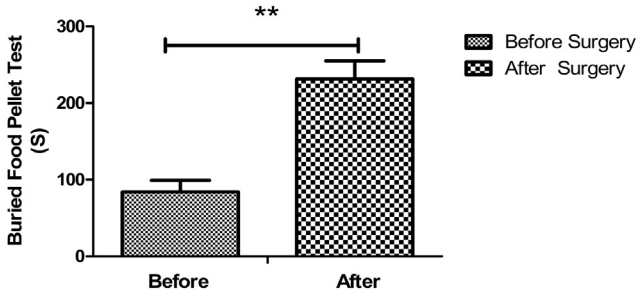

Fig. 4 The mean time (sec) of BFPT in surgery group before surgery *vs* after surgery (83.80 ± 34.37 *vs* 231.44 ± 53.23, $P < 0.05$).

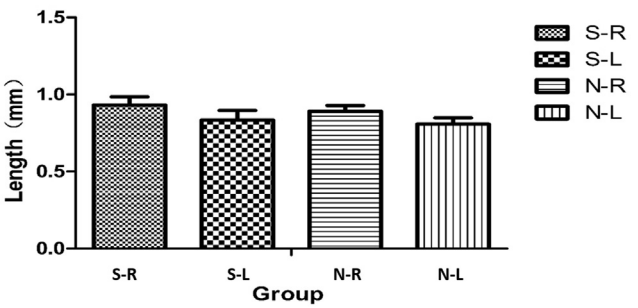

Fig. 5 Mean OF length in the control group and surgical group. S-R, S-L, N-R, N-L are the right side and left side (injury side) in the surgical group and the right side and left side in the control group, respectively. Significant difference was not observed in the OF length between the left side and right side of both groups ($P > 0.05$).

OFs with limited success. All of these methods have significant short comings, including the need to sacrifice the experimental animals, the use of potentially toxic materials, and the low resolution of the imaging methods.[15,27,47]

In this small scale study, we have demonstrated that part of the OFs can be clearly observe during MRI (Figs. 2 and 3). The method we describe could be of potential use in observing the structural integrity of rat OFs *in vivo*, both in cross-sectional and longitudinal studies. Given that MRI is one of the safest imaging modalities, it is ideal method for observing a subject without damaging the olfactory pathways or requiring sacrificing of the animal. Once a research institution has obtained a microMRI system, the examination cost is minimal.

We acknowledge that this study has several limitations. First, we cannot accurately trace the intact OFs because of their irregular shapes. The OFs shown in the figures only represent the portion of the filaments in the same coronal plane. Second, we were only able to show the oblique-coronal series images without series of axial or sagittal images, reflecting the fact that OFs are too short to be clearly observed in these planes. Lastly, we were unable to compared the MR images with the anatomy of the OF obtained via direct dissection because of the size and fragility

of the OF. Full-length imaging of the OF may require further exploration using diffusion tensor imaging (which may provide more useful information on the OFs) and other imaging methods. Clearly, this is an area ripe for additional work.

In addition to demonstrating that microMRI can visualize the OFs of rats, we showed that the blunted needle surgery procedure was effective in establishing olfactory dysfunction even when only part of the OB was damaged. A significant difference in BFPT latencies between the pre- and post-surgery measurements was observed in our study, demonstrating that even partial injury to one olfactory bulb can impair the rat's olfactory function. BFPT has been widely employed to assess the olfactory function of rats.[40,48] Another interesting finding of our study is that the blunted needle surgery did not impair the OF. This finding differs from that of some reports that use similar method to damage the OFs.[16,31,53] The main reason, in our opinion, is that the space between the OB and the cribriform plate is irregular, so the steel needle fails to completely scrape the cribriform plate, thereby sparing damage to a number of OFs. Previously researchers have tried to use a thin flexible Teflon blade to replace the steel knife to achieve this end, although in general this approach has been less successful in terms of the amount of incurred damage.[29–31] It is obvious that no matter what kind of model observed by this way, there is no doubt microMRI is an effective method to study the olfactory system including OF and OB.

OB, the first site for the processing of olfactory signal in the brain, have been repeatedly highlighted the importance for the proper functioning of olfactory system.[49–52] Our data shows, consistent with previously research, that even unilateral damage to OBs can impact normal olfactory function.

Conclusions

MicroMRI may be a feasible tool to evaluate the olfactory system including OF and OB in rat models. Unilateral partial OB lesion model is an effective post-traumatic olfactory dysfunction model.

Declaration of conflicts of interest

The authors report no conflicts of interest.

Acknowledgments

This study was supported by the National Natural Science Foundation, Government of China (No. 81670903) and the High End Foreign Expert Program (No. 20151100504).

References

1. Pinto JM. Olfaction. *Proc Am Thorac Soc*. 2011;8:46–52.
2. Wei Y, Miao X, Xian M, et al. Effects of transplanting olfactory ensheathing cells on recovery of olfactory epithelium after olfactory nerve transection in rats. *Med Sci Monit*. 2008;14: BR198–204.
3. van Riel D, Leijten LM, Verdijk RM, et al. Evidence for influenza virus CNS invasion along the olfactory route in an immunocompromised infant. *J Infect Dis*. 2014;210:419–423.
4. van Riel D, Verdijk R, Kuiken T. The olfactory nerve: a shortcut for influenza and other viral diseases into the central nervous system. *J Pathol*. 2015;235:277–287.
5. Zhang C, Chen J, Feng C, et al. Intranasal nanoparticles of basic fibroblast growth factor for brain delivery to treat Alzheimer's disease. *Int J Pharm*. 2014;461:192–202.
6. Kozlovskaya L, Abou-Kaoud M, Stepensky D. Quantitative analysis of drug delivery to the brain via nasal route. *J Control Release*. 2014;189:133–140.
7. Patchin ES, Anderson DS, Silva RM, et al. Size-dependent deposition, translocation, and microglial activation of inhaled silver nanoparticles in the rodent nose and brain. *Environ Health Perspect*. 2016;124:1870–1875.
8. Pardeshi CV, Belgamwar VS. Direct nose to brain drug delivery via integrated nerve pathways bypassing the blood-brain barrier: an excellent platform for brain targeting. *Expert Opin Drug Deliv*. 2013;10:957–972.
9. Dhuria SV, Hanson LR, Frey WH. Intranasal delivery to the central nervous system: mechanisms and experimental considerations. *J Pharm Sci*. 2010;99:1654–1673.
10. Graziadei PP. Cell dynamics in the olfactory mucosa. *Tissue Cell*. 1973;5:113–131.
11. Masukawa LM, Hedlund B, Shepherd GM. Changes in the electrical properties of olfactory epithelial cells in the tiger salamander after olfactory nerve transection. *J Neurosci*. 1985;5: 136–141.
12. Yee KK, Costanzo RM. Changes in odor quality discrimination following recovery from olfactory nerve transection. *Chem Senses*. 1998;23:513–519.
13. Yee KK, Rawson NE. Retinoic acid enhances the rate of olfactory recovery after olfactory nerve transection. *Brain Res Dev Brain Res*. 2000;124:129–132.
14. Yamasaki A, Sugahara K, Takemoto T, Ikeda T, Yamashita H. Effect of Ninjin-yoei-to (Rensheng-Yangrong-Tang) on olfactory behavior after olfactory nerve transection. *Phytomedicine*. 2008;15:358–366.
15. Kobayashi M, Tamari K, Miyamura T, Takeuchi K. Blockade of interleukin-6 receptor suppresses inflammatory reaction and facilitates functional recovery following olfactory system injury. *Neurosci Res*. 2013;76:125–132.
16. Al SMO, Kobayashi M, Tamari K, Miyamura T, Takeuchi K. Tumor necrosis factor-α antagonist suppresses local inflammatory reaction and facilitates olfactory nerve recovery following injury. *Auris Nasus Larynx*. 2017;44:70–78.
17. Bakos SR, Costanzo RM. Matrix metalloproteinase-9 is associated with acute inflammation after olfactory injury. *Neuroreport*. 2011;22:539–543.
18. Bakos SR, Schwob JE, Costanzo RM. Matrix metalloproteinase-9 and -2 expression in the olfactory bulb following methyl bromide gas exposure. *Chem Senses*. 2010;35:655–661.
19. El-Habashi N, el-S E, Fukushi H, et al. Experimental intranasal infection of equine herpesvirus 9 (EHV-9) in suckling hamsters: kinetics of viral transmission and inflammation in the nasal cavity and brain. *J Neurovirol*. 2010;16:242–248.
20. Frontera JL, Raices M, Cervino AS, Pozzi AG, Paz DA. Neural regeneration dynamics of Xenopus laevis olfactory epithelium after zinc sulfate-induced damage. *J Chem Neuroanat*. 2016; 77:1–9.
21. Ueha R, Ueha S, Kondo K, et al. Damage to olfactory progenitor cells is involved in cigarette smoke-induced olfactory dysfunction in mice. *Am J Pathol*. 2016;186:579–586.
22. Turner JH, May L, Reed RR, Lane AP. Reversible loss of neuronal marker protein expression in a transgenic mouse model for sinusitis-associated olfactory dysfunction. *Am J Rhinol Allergy*. 2010;24:192–196.

23. Holbrook EH, Leopold DA, Schwob JE. Abnormalities of axon growth in human olfactory mucosa. *Laryngoscope*. 2005;115: 2144—2154.
24. Meredith M, RJO. HRP uptake by olfactory and vomeronasal receptor neurons: use as an indicator of incomplete lesions and relevance for non-volatile chemoreception. *Chem Senses*. 1988;13:487—515.
25. Chuang KH, Lee JH, Silva AC, Belluscio L, Koretsky AP. Manganese enhanced MRI reveals functional circuitry in response to odorant stimuli. *Neuroimage*. 2009;44:363—372.
26. David CD, Melanie LF. Olfactory transport of manganese: implications for neurotoxicity. In: Costa L, Aschner M, eds. *Manganese in Health and Disease*. New Jersey, NJ: Humana Press, Inc; 2014:119—127.
27. Crossgrove J, Zheng W. Manganese toxicity upon overexposure. *NMR Biomed*. 2004;17:544—553.
28. Shiga H, Kinoshita Y, Washiyama K, et al. Odor detection ability and thallium-201 transport in the olfactory nerve of traumatic olfactory-impaired mice. *Chem Senses*. 2008;33:633—637.
29. Costanzo RM. Rewiring the olfactory bulb: changes in odor maps following recovery from nerve transection. *Chem Senses*. 2000;25:199—205.
30. Kobayashi M, Costanzo RM. Olfactory nerve recovery following mild and severe injury and the efficacy of dexamethasone treatment. *Chem Senses*. 2009;34:573—580.
31. Costanzo RM, Perrino LA, Kobayashi M. Response of matrix metalloproteinase-9 to olfactory nerve injury. *Neuroreport*. 2006;17:1787—1791.
32. Shiga H, Taki J, Yamada M, et al. Evaluation of the olfactory nerve transport function by SPECT-MRI fusion image with nasal thallium-201 administration. *Mol Imaging Biol*. 2011;13: 1262—1266.
33. Lauterbur PC. Image formation by induced local interactions. Examples employing nuclear magnetic resonance. *Clin Orthop Relat Res*. 1973;1989:3—6.
34. Chang C, Jang T. Magnetic resonance microscopy of hamster olfactory bulb: a histological correlation. *Anat Rec*. 1995;242: 132—135.
35. Alberts JR, Galef BG. Acute anosmia in the rat: a behavioral test of a peripherally-induced olfactory deficit. *Physiol Behav*. 1971;6:619—621.
36. Yang M, Crawley JN. *Simple Behavioral Assessment of Mouse Olfaction. Curr Protoc Neurosci*. New York John Wiley & Sons, Inc; 2009, 8.24.1—8.24.12.
37. Witt RM, Galligan MM, Despinoy JR, Segal R. Olfactory behavioral testing in the adult mouse. *J Vis Exp*. 2009;23:949.
38. Getchell TV, Kwong K, Saunders CP, Stromberg AJ, Getchell ML. Leptin regulates olfactory-mediated behavior in ob/ob mice. *Physiol Behav*. 2006;87:848—856.
39. Del PK, Leinders-Zufall T, Rodriguez I, et al. Deficient pheromone responses in mice lacking a cluster of vomeronasal receptor genes. *Nature*. 2002;419:70—74.
40. Ye J, He JP, Liu ZJ. Olfactory mucosal microstructural changes in a rat model of acute rhinosinusitis with dysosmia. *Genet Mol Res*. 2014;13:3859—3868.
41. Hopkins LE, Patchin ES, Chiu PL, Brandenberger C, Smiley-Jewell S, Pinkerton KE. Nose-to-brain transport of aerosolised quantum dots following acute exposure. *Nanotoxicology*. 2014; 8:885—893.
42. Pan L, Zhou J, Ju F, Zhu H. Intranasal delivery of α-asarone to the brain with lactoferrin-modified mPEG-PLA nanoparticles prepared by premix membrane emulsification. *Drug Deliv Transl Res*. 2018;8:83—96.
43. Tjälve H, Henriksson J. Uptake of metals in the brain via olfactory pathways. *Neurotoxicology*. 1999;20:181—195.
44. Reden J, Mueller A, Mueller C, et al. Recovery of olfactory function following closed head injury or infections of the upper respiratory tract. *Arch Otolaryngol Head Neck Surg*. 2006;132: 265—269.
45. Jiang RS, Twu CW, Liang KL. Medical treatment of traumatic anosmia. *Otolaryngol Head Neck Surg*. 2015;152:954—958.
46. Delank KW, Fechner G. Pathophysiology of post-traumatic anosmia. *Laryngorhinootologie*. 1996;75:154—159.
47. Gobbo OL, Petit F, Gurden H, Dhenain M. In vivo detection of excitotoxicity by manganese-enhanced MRI: comparison with physiological stimulation. *Magn Reson Med*. 2012;68:234—240.
48. Zhang Q, Yan W, Bai Y, Zhu Y, Ma J. Repeated formaldehyde inhalation impaired olfactory function and changed SNAP25 proteins in olfactory bulb. *Int J Occup Environ Health*. 2014;20: 308—312.
49. Breton-Provencher V, Lemasson M, Peralta MR, Saghatelyan A. Interneurons produced in adulthood are required for the normal functioning of the olfactory bulb network and for the execution of selected olfactory behaviors. *J Neurosci*. 2009;29: 15245—15257.
50. Gheusi G, Cremer H, McLean H, Chazal G, Vincent JD, Lledo PM. Importance of newly generated neurons in the adult olfactory bulb for odor discrimination. *Proc Natl Acad Sci U S A*. 2000;97:1823—1828.
51. Lin DY, Zhang SZ, Block E, Katz LC. Encoding social signals in the mouse main olfactory bulb. *Nature*. 2005;434:470—477.
52. Mori K, Nagao H, Yoshihara Y. The olfactory bulb: coding and processing of odor molecule information. *Science*. 1999;286: 711—715.
53. Mansoor AK, Thomas S, Sinha JK, Alladi PA, Ravi V, Raju TR. Olfactory tract transection reveals robust tissue-level plasticity by cellular numbers and neurotrophic factor expression in olfactory bulb. *Indian J Exp Biol*. 2012;50:765—770.

Edited by Yi Fang